Back-Face Strain Compliance Calibration for the Four-Point Bend Specimen

Yong-Hak Huh*
Material Evaluation Center, Korea Research Institute of Science and Standards
Ji-Ho Song
Department of Mechanical Engineering, Korea Advanced Institute of Science and Technology

Back-face strain compliance (BFS compliance) for the four-point bend specimen has been calibrated for various crack length ratios. Finite element technique was employed to simulate four-point loading and calculate back-face strain of the bend specimen. The numerically determined strain variation along the back face indicates that the sensitivity to gage placement increases with crack length and back-face strain at the gage length less than 0.2W, where W is the width of the bend specimen, can be measured within 5% deviation of the maximum BFS. Non-dimensional back-face strain compliance, $-E'BCW$, was calibrated with FE analysis and experiment. The experimentally determined compliance indicates good agreement with the numerical compliance and can be expressed as a function of crack length ratio.

Key Words: Back-Face Strain Compliance, Four-Point Bend Specimen, COD, Calibration

Nomenclature

a/W	: Crack length ratio
BFS	: Back-face strain
C	: The elastic compliance defined as $-\varepsilon W/M$ for the four-point bending specimen
K	: Stress intensity factor
$E'BW\delta/M$	: Non-dimensional COD (crack opening displacement) compliance
$E'BCW$	: Non-dimensional back-face strain compliance
U	: The inverse back-face strain compliance defined as $1/\sqrt{E'BCW+1}$
δ	: Crack opening displacement
4PB	: Four-point bend

* Corresponding Author,
E-mail : yhhuh@kriss.re.kr
TEL : +82-42-868-5386 ; **FAX** : +82-42-868-5032
Material Evaluation Center, Korea Research Institute of Science and Standards, Science Town, Taejon 305-600, Korea. (Manuscript **Received** June 9, 1999; **Revised** December 6, 1999)

1. Introduction

Stiffness of a specimen in mechanics of materials testing can be simply obtained by measuring two basic physical quantities; namely, applied load and specimen deformation (or displacement). The inverse of the stiffness represents the compliance, which is defined as the displacement per unit load. The variation in the compliance value depends on the geometry of the specimen and the size of the defect contained in it. Using this dependency, the compliance technique has been used as one of the methods for evaluation of crack length in material testing. In addition, this technique can be easily utilized where it is not easy to directly measure the crack length, or continuous data should be acquired automatically.

Back-face strain represents the strain measured at the opposite face from where the notch is machined. The back-face strain compliance was defined from the relationship between the load and back-face strain. (Deans and Richards, 1979) Since this suggestion, back-face elastic strain

(BFS) compliance technique has been widely used in many material tests. Deans and Richards (1979) defined the BFS compliance as a function of crack length in CT (compact tension) specimen. Gilbert *et al.* (1994) calculated the BFS compliance function in DCT(disk-shaped compact tension) specimen by an experiment and numerical analysis. The BFS compliance technique has been used in monitoring the crack length (Shaw and Zhao, 1994, Ritchie *et al*, 1989, Richards and Deans, 1980) and determining the fatigue crack closure level for these specimens (Ritchie and Yu, 1986, Huh *et al*, 1997). And, recently, this technique was employed in assessing the magnitude of crack bridging effects, which result from the interaction between the matrix and grains at the cracked ligament, in the wake of crack tip(Ritchie *et al*, 1989)

The four-point bend specimen (4PB specimen) has the central area in which the bending moment is uniform, and, therefore, is one of the popularly used specimens for fatigue crack growth testing. Especially, the configuration of the 4PB specimen has been widely used for fracture and fatigue testing of ceramics that have some difficulties in machining. However, BFS compliance calibration for the 4PB specimen has not been reported. Therefore, in this study, the BFS compliance was calibrated for the 4PB specimen by employing the finite element technique and experiment. The sensitivity to the gage placement along the back -face of the specimen was investigated and the gage length optimal to minimize the deviation in measurement of the back-face strain was also suggested.

2. Numerical Method and Experimental Procedures

Figure 1 shows the geometry and loading configuration of the 4PB specimen used in this study. As shown in the figure, major and minor span of the specimen are taken equal to 6W and 4W, respectively, where W is the width of the specimen. To determine the sensitivity to gage placement along the back face and to calculate the BFS compliance values, the linear-elastic, plane strain,

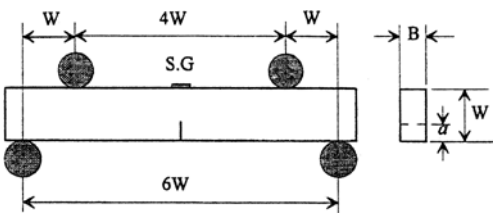

Fig. 1 Geometric shape and dimension of the four-point bend specimen for FE analysis and experiment (W=6mm, B=3mm)

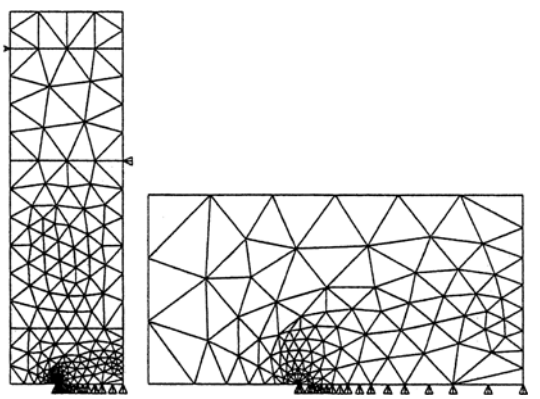

(a) Global mesh (b) Mesh near crack tip

Fig. 2 Typical mesh used in finite element analysis

finite element analysis was carried out. A commercial finite element code, ANSYS 5. 0, was used in the analysis. Two-dimensional half-model of the specimen was meshed with six-noded isoparametric triangular elements. Region in the immediate vicinity of the crack tip was modeled with refined meshes and singular elements. To accommodate square-root strain singularity near crack tip, the mid-side nodes in the singular elements are moved to quarter point positions. Specimens with 10 different values of crack length ratio, a/W, ranged from 0. 15 to 0. 6, were modeled. Figure 2 shows the mesh generated over the specimen and near crack tip at a/W =0.4.

Material properties used for the analysis are as follows: Young's modulus E=390GPa, Poisson's ratio, ν=0.25. These properties correspond to those of alumina ceramic used in this experiment.

To measure the BFS compliance in experiment, the 4PB specimens similar to the geometry shown

in Fig. 1 were machined using alumina ceramics (Al_2O_3). Thickness, B, and width, W, of the specimen were 3 and 6 mm, respectively. A straight V-typed notch at the mid-plane of the specimen was machined. Root angle of the notch was 20°. The 8 different lengths of the notch, ranged from a/W=0. 15 to 0. 6, were ground. Values of the BFS compliance at the respective crack lengths were determined from the load-subtracted back-face strain curve obtained under cyclic loading. Back-face strain was measured from a strain gage mounted at the back face of the specimen, centered along its mid plane. Gage length and resistivity of the strain gage were 1mm and 120Ω, respectively.

3. Results and discussion

3.1 Crack opening displacement compliance

The 4PB configuration used in this study may be represented as the limiting case of a pure bend situation as the major and minor span are 6W and 4W, respectively. For the pure bend configuration, crack opening displacement, δ, is given by

$$\delta = 24\frac{Ma}{E'BW^2}f(\alpha) \tag{1}$$

where M and α are the bending moment and crack length ratio, a/W, respectively. The non-dimensional geometrical function $f(\alpha)$ was expressed by Tada *et al.*(1973) as

$$f(\alpha) = 0.8 - 1.7\alpha - 2.4\alpha^2 + \frac{0.66}{(1-\alpha)^2} \tag{2}$$

and by Murakami (1987) as

$$f(\alpha) = 1.458 - 0.304\alpha - 0.924\alpha^2 + 48.34\alpha^3 - 123.5\alpha^4 + 120.5\alpha^5 \tag{3}$$

Crack opening displacement, δ, given as eq. (1), can be restated as follows:

$$\frac{E'BW\delta}{M} = 24\frac{a}{W}f(\alpha) \tag{4}$$

Equation (4) is a normalized form of the crack opening displacement and can be stated as non-dimensional COD(crack opening displacement) compliance. As can be found from Eq. (4), values of COD compliance can be represented as a function of crack length ratio, a/W. Thus, the COD compliance data can be obtained for the respective cases represented by Eqs. (2) and (3).

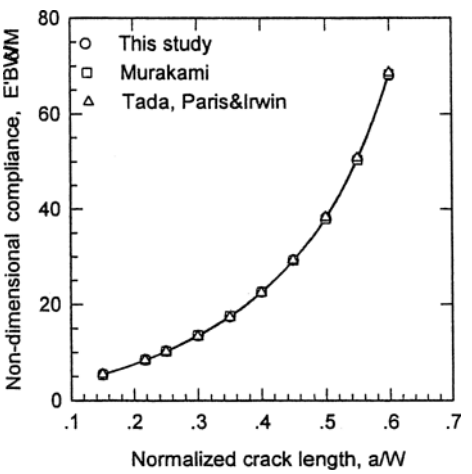

Fig. 3 Variation of non-dimensional COD compliance with crack length

By performing the numerical analysis, in this study, the COD compliance values for the various crack length ratios were calculated. The compliance data obtained numerically was compared to the data given by Eqs. (2) and (3) to confirm the confidence in this numerical analysis. These values are plotted in Fig. 3, together with the COD compliance relations given by Eqs. (2) and (3). The correlation between the compliance data obtained numerically and analytically is very good. Therefore, it indicates that the mesh generation of the specimen used in this analysis was well optimized.

3.2 Distribution of back-face strain

From the numerical analysis for the specimens with the various crack lengths, the distribution of strain over the specimen was obtained. Figure 4 shows an example among the various cases obtained in this study, where the crack length ratio, a/W, and the stress intensity factor, K, are 0.4 and 3.2 MPa $m^{1/2}$, respectively. In Figs. 4(a) and (b), stress distribution near crack tip and strain distribution over the specimen are shown, respectively. The compressive strain was distributed along the back face of the specimen and the magnitude of the strain decreased with the distance from the centerline of the back face. Thus,

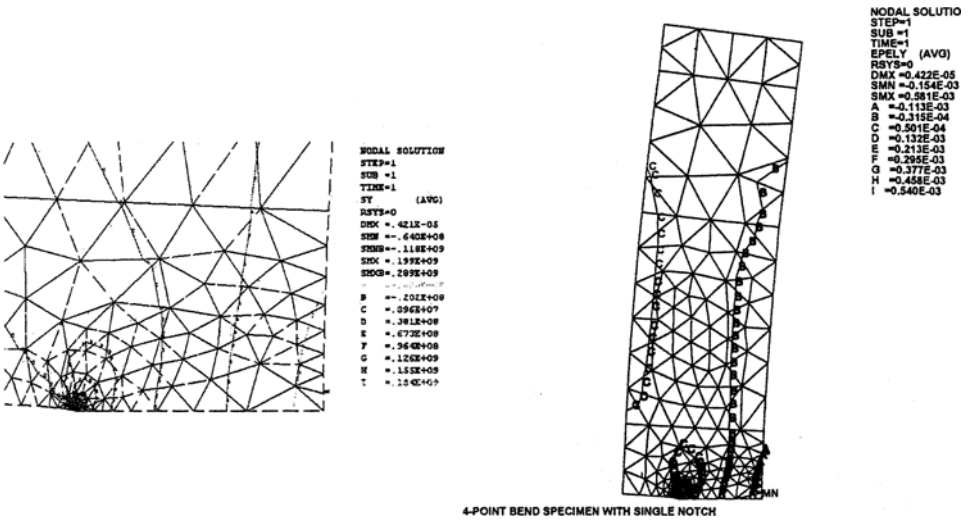

(a) Stress distribution near crack tip (b) Strain distribution over the specimen

Fig. 4 Distribution of strain over the 4PB specimen with crack ratio, a/W, of 0.4 for K=3.2MPa $m^{1/2}$

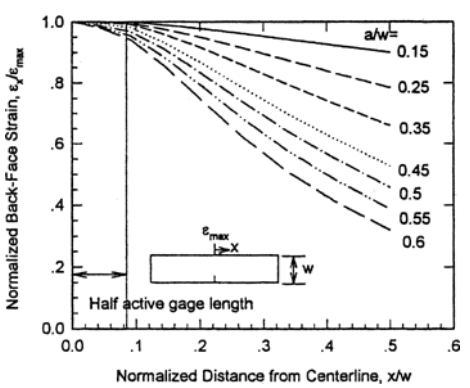

Fig. 5 Gradient of back-face strain along the back face at various crack ratios

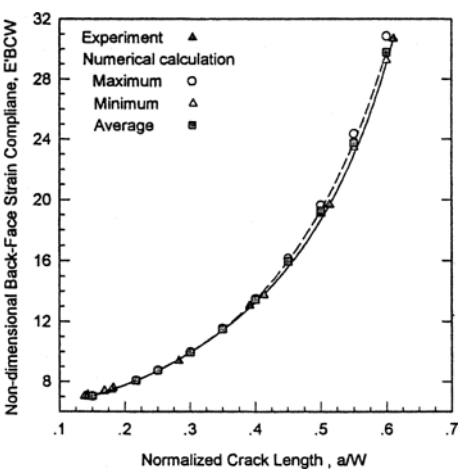

Fig. 6 Variation of non-dimensional back-face strain compliance obtained from experiment and FE analysis with crack length

the gradient of the back-face strain may affect the sensitivity to the gage size and placement along the back face.

Figure 5 shows the variation in the back-face strain with the distance from the centerline at the various crack length ratios. In this figure, the back-face strain, ε, and the distance, x, were normalized with the maximum values of the back-face strain, ε_{max}, and the width of the specimen, W, respectively. The normalized back-face strain, $\varepsilon/\varepsilon_{max}$, decreases with increase of the distance from the center line. And also, the gradient of the back-face strain depends on the crack length, indicating that the sensitivity to gage placement increases with crack length. For a/W =0.6, the variation of the normalized back-face strain increased to less than 5% of the maximum value at the normalized distance, x/W, of 0.1. Thus, it can be said that experimental measurement of the back-face strain within the range of the gage length of 0.2W may be reasonably insensitive to gage placement.

Table 1 Back-face compliance function

$E'BCW = \alpha_0 + \alpha_1(a/W) + \alpha_2(a/W)^2 + \alpha_3(a/W)^3 + \alpha_4(a/W)^4 + \alpha_5(a/W)^5 + \alpha_6(a/W)^6$

Degree, i	Coefficient, α_i
0	7.2048
1	-11.9072
2	78.0932
3	-0.0347
4	-109.0541
5	-60.5026
6	422.3264

3.3 Calibration of back-face strain compliance

Figure 6 shows the back-face strain (BFS) compliance obtained numerically and experimentally. In this figure, the BFS compliance is presented as the non-dimensional strain compliance function, E'BCW, as a function of the normalized crack length, a/W. Here, the compliance function is normalized by the Young's modulus, $E'(=E/(1-\nu^2))$, thickness, B, and width, W. C is an elastic compliance, defined as $-\varepsilon W/M$, where M is applied moment and ε is the back-face strain. The BFS compliance was calibrated in the form of the normalized compliance. Fitting a polynomial by the least square technique to the experimentally obtained compliance values, the corresponding calibration function is obtained as given in Table 1. A sixth-degree polynomial was used to represent the function as the fitting error was found to be sufficiently small and relative improvement was not found with the increment of the polynomial order. This calibration function describes the compliance data in error within less than 1%.

For practical use, the back-face strain compliance function may be used in the compliance crack length relation. The relation for the 4PB specimen can be expressed in the form given as

$$\frac{a}{W} = f(E'BCW), \tag{5}$$

where $E'BCW$ is the back-face strain compliance defined above. According to the proposal by Saxena and Hudak(1978), the relation, given as Eq. (5), can be rewritten in the form

Table 2 Inverse back-face strain compliance function

$a/W = \beta_0 + \beta_1 U + \beta_2 U^2 + \beta_3 U^3 + \beta_4 U^4 + \beta_5 U^5 + \beta_6 U^6$

where $U = \frac{1}{\sqrt{E'BCW + 1}}$

Degree, i	Coefficient, α_i
0	1.07193
1	-3.00967
2	0.1064
3	0.048072
4	0.095537
5	-1.06943
6	-271.3686

$$\frac{a}{W} = g(U) \tag{6}$$

where $U = \frac{1}{\sqrt{E'BCW + 1}}$ (7)

The polynomial function, g, was also fitted by least square technique to the data corresponding to Eq. (6). The coefficients of the function are listed in Table 2.

BFS compliance values obtained by numerical analysis are plotted in Fig. 6, together with those by experiment. The gradient in the compliance, as shown in Fig. 5, may result in the different compliance values with the distance from the centerline. Thus, the maximum, the minimum and average values of the compliance within the range of the gage length are presented in Fig. 6. The correlation between the experimental and numerical values of the compliance looks relatively good. The difference between the average values, obtained in numerical analysis, and the experimental fitting curve was less than 3% in the range of crack length ratio, a/W, from 0.15 to 0.5, but increased to 3.6% for the crack length ratio of 0.6. This increment of the difference with the increase of the crack length may be caused to the increased sensitivity to the gage placement.

4. Summary and Conclusions

Back-face strain compliance calibration for the four-point bend specimen has been carried out. The back-face strain compliance function was

presented as a sixth-degree polynomial of crack length ratio. Numerically and experimentally obtained back-face strain compliance agreed very well for values of crack length ratio less than 0.6. An increased difference between experimental and numerical values of the compliance was observed at larger values of crack length ratio, which may be caused by the increased sensitivity to the gage placement. An increasingly steep strain gradient along the back face with crack length was shown. This indicated that the sensitivity to gage placement increases with crack length and the gage length less than 0.2W is optimal for measurement of BFS within 5% deviation of the maximum BFS.

References

Deans, W.F. and Richards C.E., 1979, "A Simple and Sensitive Method of Monitoring Crack and Load in Compact Fracture Mechanics Specimens using Strain Gages," *JTEVA*, Vol. 7, No. 3, pp. 147~154

Gilbert, C.J., McNaney, J.M., Dauskardt, R.H., and Ritchie, R. O., 1994, "Back-Face Strain Compliance and Electrical-Potential Crack Length Calibrations for the Disc-Shaped Compact-Tension DC(T) Specimen," *JTEVA*, Vol. 22, No. 2, pp. 117~120

Huh, Y.H., Cho, S.J., Yoon, K.J., and Song, J. H., 1997, "Fatigue Crack Growth in SiC Ceramics under Cyclic Loading," *Proceedings of KSME 2nd Material and Fracture Division Conference*, pp. 79~84

Murakami, Y., 1987, *Stress Intensity Factors Handbook*, *JSMS*, Pergamon Press

Richards, C.E. and Deans, W.F., 1980, "The Measurement of Crack Length and Load using Strain Gauges, in *The Measurement of Crack Length and Shape during Fracture and Fatigue*, *EMAS*, pp. 28~68

Ritchie, R.O, Yu, W. and Bucci, R.J., 1989, "Fatigue Crack Propagation in ARALL Laminates: Measurement of the Effect of Crack Tip Shielding From Crack Bridging, Eng." *Fract. Mech.*, Vol. 32, No. 3, pp. 361~377

Ritchie, R.O., and Yu, W., 1986, "Short Crack Effects in Fatigue: A Consquence of Crack Tip Shielding, in Small Fatigue Cracks," R.O. Ritchie and J. Lankford, Eds., *The Metallurgical Society of the American Institute of Mining, Metallurgical and Petroleum Engineers*, Warrendale, PA, pp. 167~189

Saxena, A., and Hudak, Jr., S. J., 1978, "Review and Extension of Compliance information for Common Crack Growth Specimens," *Int. J. Fracture* 14, 453~468

Shaw, W.J.D. and Zhao, W., 1994, "Back Face Strain Calibration for Crack Length Measurements," *JTEVA*. Vol. 22, No. 6, pp. 512~516

Tada, H., Paris, P., and Irwin, G., 1973, *The Stress Analysis handbook*, Del Research Corp., Hellerstown, PA, 2.13~2.15